Neoplasia • Vol. 7, No. 3, March 2005, pp. 280–293 280

www.neoplasia.com

Inverse Relationship between 15-Lipoxygenase-2 and PPAR-γ Gene Expression in Normal Epithelia Compared with Tumor Epithelia[1]

Vemparala Subbarayan, Xiao-Chun Xu*, Jeri Kim†, Peiying Yang‡, Ashraful Hoque*, Anita L. Sabichi*, Norma Llansa*, Gabriella Mendoza*, Christopher J. Logothetis†, Robert A. Newman‡, Scott M. Lippman* and David G. Menter**

Departments of *Clinical Cancer Prevention, †Genitourinary Medical Oncology and ‡Experimental Therapeutics, The University of Texas M. D. Anderson Cancer Center, Houston, TX 77030, USA

Abstract

15-Lipoxygenase-2 (15-LOX-2) synthesizes 15-*S*-hydroxyeicosatetraenoic acid (15-*S*-HETE), an endogenous ligand for the nuclear receptor, peroxisome proliferator–activated receptor-γ (PPAR-γ). Several studies have described an inverse relationship between 15-LOX-2 and PPAR-γ expression in normal *versus* tumor samples. To systematically determine if this is a ubiquitous phenomenon, we used a variety of epithelial and nonepithelial cells and some tissues to further evaluate the extent of this inverse relationship. The levels of mRNA or protein were measured by reverse transcriptase polymerase chain reaction or Western gray level intensity, whereas distribution was determined by *in situ* hybridization or immunofluorescence. 15-*S*-HETE was measured by liquid chromatography/tandem mass spectrometry. Normal epithelial cells/samples generally expressed high levels of 15-LOX-2 along with the enzyme product 15-*S*-HETE, but both levels were reduced in cancer cells/samples. In contrast, most cancer cells expressed high levels of PPAR-γ mRNA and protein, which were absent from normal epithelial cells. Overall, the inverse relationship between these two genes was primarily restricted to epithelial samples. Forced expression of PPAR-γ reduced 15-LOX-2 protein levels in normal cells, whereas forced expression of 15-LOX-2 in tumor cells suppressed PPAR-γ protein levels. These results suggest that feedback mechanisms may contribute to the loss of 15-LOX-2 pathway components, which coincide with an increase in PPAR-γ in many epithelial cancers.

Neoplasia (2005) **7,** 280–293

Keywords: 15-lipoxygenase, prostate cancer, gene expression, peroxisome proliferator–activated receptor-γ, PPAR-γ.

Introduction

Lipoxygenase (LOX) enzymes catalyze the conversion of polyunsaturated fatty acids to hydroxy fatty acids [1,2]. LOX enzymes contain a nonheme iron (Fe^{3+}) that promotes hydrogen abstraction and dioxygenation of 1,4-diene moieties, followed by protonation of the peroxyl radical to form monohydroperoxy fatty acids predominantly from mobilized lipid pools [2–4]. A wide variety of LOXs are found in nature, which are described based on the carbon atom that each enzyme peroxygenates on a particular substrate [2–4]. The primary lipid targets of LOX activity are arachidonic acid (AA) and linoleic acid (LA). Two forms of 15-LOX occur in humans: 15-lipoxygenase-1 (15-LOX-1), originally isolated from reticulocytes [5], and 15-lipoxygenase-2 (15-LOX-2), first described in skin [6]. 15-LOXs are distinguished by their catalytic properties. 15-LOX-2 preferentially peroxidates AA on carbon 15 to generate 15-*S*-hydroperoxyeicosatetraenoic acid, which is hydrolyzed to 15-*S*-hydroxyeicosatetraenoic acid (15-*S*-HETE) [3,6]. In contrast, 15-LOX-1 preferentially peroxidates LA on carbon 13 to form 13-*S*-hydroperoxyoctadecadienoic acid, which is hydrolyzed to 13-*S*-hydroxyoctadecadienoic acid (13-*S*-HODE) [7]. 15-LOX-1 also generates 15-*S*-hydroperoxyeicosatetraenoic acid from AA (thus the nomenclature), but less efficiently than 15-LOX-2 [7]. A variety of oxidized lipids, including 15-*S*-HETE, can activate the nuclear receptor peroxisome proliferator–activated receptor γ (PPAR-γ) during inflammation and prostate cancer [8–11].

15-LOX-2 expression is most studied in human prostate, a tissue initially reported to have one of the highest expression levels of this gene [6]. Shappell et al. [12] reported that 15-LOX-2 expression was high in benign prostatic epithelium, but was low in malignant prostatic adenocarcinoma. Tang et al. [13] reported that 15-LOX-2 levels were high in normal

Abbreviations: AA, arachidonic acid; LA, linoleic acid; 15-LOX-1, 15-lipoxygenase-1; 15-LOX-2, 15-lipoxygenase-2; 15-*S*-HETE, 15-*S*-hydroxyeicosatetraenoic acid; PPAR, peroxisome proliferator–activated receptor; 13-*S*-HODE, 13-S-hydroxyeicosatetraenoic acid; IgG, immunoglobulin G; RT-PCR, reverse transcriptase polymerase chain reaction; BSA, bovine serum albumin; PBS, phosphate-buffered saline; DAPI, 4′,6-diamidino-2-phenylindole dilactate; LC/MS/MS, liquid chromatography/tandem mass spectrometry; ISH, *in situ* hybridization

Address all correspondence to: David G. Menter, Department of Clinical Cancer Prevention, Box 236, The University of Texas M. D. Anderson Cancer Center, 1515 Holcombe Boulevard, Houston, TX 77030. E-mail: dmenter@mdanderson.org

[1]This work was supported by grant TPRN-99-240-01-CNE-1 from the American Cancer Society and by National Cancer Institute grants P01 CA-91844, P50 CA90270, 1 R21 CA102145, and K12 CA-88084.

Received 1 July 2004; Revised 25 August 2004; Accepted 1 September 2004.

DOI 10.1593/neo.04457

prostatic epithelial cells and, when expressed, also acted as negative cell cycle regulator. Further work by Bhatia et al. [14] suggested that tumor-suppressive functions of 15-LOX-2 may not necessarily depend solely on AA-metabolizing activity or localization to the nucleus. Jack et al. [15] also correlated 15-LOX-2 levels with tumor grade (> 5 Gleason score); expression was reduced in higher-grade tumors. Moreover, 15-LOX-2 expression was significantly reduced in high-grade prostatic intraepithelial neoplasia compared with benign tissue [15]. In addition, 15-*S*-HETE production was lower in prostatic adenocarcinoma compared with benign prostatic hyperplasia, which produced both 15-LOX-2 and 15-*S*-HETE [8,12]. These studies suggest that the loss of the 15-LOX-2 pathway may contribute to increased proliferation and reduced differentiation in prostatic adenocarcinoma.

In view of what is known about 15-LOX-2 expression in prostate and the limited information available for other tissues, we examined the expression of 15-LOX-2 and its relationship with PPAR-γ expression in normal or cancer samples from various epithelial and nonepithelial sources. We hypothesized that an inverse relationship exists between 15-LOX-2 and PPAR-γ expression in normal samples compared to tumor samples, which may be a generalized phenomenon. As an extension of this hypothesis, we also hypothesized that complex mechanisms limit the coexpression of 15-LOX-2 pathway components and PPAR-γ in cells, particularly in the presence of substrate or ligand. We set out to determine if an inverse relationship between these two genes was common to epithelial tissues. We also determined whether forced expression of either 15-LOX-2 or PPAR-γ would affect the endogenous expression of its counterpart, or be altered by AA or 15-*S*-HETE. Based on these outcomes, we might expect that disrupting the counterregulation of 15-LOX-2 or PPAR-γ would profoundly influence epithelial carcinogenesis.

Materials and Methods

The primary rabbit antibody against 15-LOX-2 was purchased from Oxford Biomedical Research, Inc. (Oxford, MI). Primary antibodies against PPAR-γ [rabbit polyclonal immunoglobulin G (IgG) and mouse monoclonal IgG_1] were purchased from Santa Cruz Biotechnology, Inc. (Santa Cruz, CA). The secondary antibodies to rabbit, or mouse IgG that were conjugated to horseradish peroxidase, were obtained from Pierce Chemical Co. (Rockford, IL), or those conjugated to Alexa-488 were purchased from Molecular Probes (Eugene, OR). Deuterated liquid chromatography/tandem mass spectrometry (LC/MS/MS) standard, 15-*S*-HETE-d_8, and purified 15-*S*-HETE were purchased from Cayman Chemical Co. (Ann Arbor, MI). AA and butylated hydroxytolulene (BHT) were obtained from Sigma Chemical Co. (St. Louis, MO).

Cell Culture

Tumor cell lines derived from different epithelial and nonepithelial origins were grown in tissue culture. The cells of normal epithelial origin included normal prostate epithelial cells (PrEC), normal or immortalized normal keratinocytes (NHEK and NK), human bronchial epithelial cells (NHBE), human mammary epithelial cells (HMEC), and immortalized normal bladder cells (SVHUC), which were purchased from Cambrex BioScience (Walkersville, MD) or American Tissue Type Culture Collection (ATCC; Manassas, VA). Normal esophageal epithelial cells (EEC) were obtained from the Department of Surgery and Surgical Basic Science, Graduate School of Medicine, Kyoto University (Kyoto, Japan). Esophageal cancer cell lines TE-3 and TE-12 were obtained from the First Department of Pathology, Hiroshima University School of Medicine (Hiroshima, Japan). Skin squamous cell carcinomas (HaCaT, SCC-M7, and SCC-P9) were provided by Dr. John Clifford (Lousiana State University, Shreveport, LA). UM-UC-9 and UM-UC-14 bladder cells, referred to hereafter as U-9 and U-14 were obtained from Dr. Barton Grossman at The University of Texas M.D. Anderson Cancer Center. Other cancer cells were obtained from ATCC, including breast carcinoma cells (MCF-7, SK-BR-3, and MDA-MB-453), pancreatic carcinoma cells (AsPC-1, MIA PaCa, and Panc 28), colon carcinoma cells (HCT-115, SW-480, and SW-620), and prostate carcinoma cells (PC-3, LnCaP, and DU 145). Hepatic carcinoma cells (Hep 3B and Hep G2) cells were purchased from ATCC. The cells from nonepithelial origin including prostate stromal cells (PrSt) and prostate smooth muscle cells (PrSM) were purchased from Cambrex BioScience. NIH-3T3 cells were also purchased from ATCC. Also, cells from neuroepithelial or neural crest origins, melanocytes Cambrex BioScience, and melanoma cells (MeWo, 3S5, and 70W) were obtained from Dr. Robert Kerbel, Sunnybrook and Women's College Health Sciences Centre in Toronto, Ontario, Canada. Primary cell cultures were maintained in defined culture medium according to the manufacturer's instructions as described previously [16]. Cancer cell lines were maintained in Dulbecco's modified Eagle's medium/F-12 low-glucose medium (Invitrogen-GIBCO, Carlsbad, CA) supplemented with 5% to 10% fetal bovine serum.

Reverse Transcriptase Polymerase Chain Reaction (RT-PCR)

Total RNA was extracted using RNA STAT-60 reagent (Tel-Test, Inc., Friendswood, TX) and treated with DNase I before use in RT-PCR. One microgram of RNA was reverse-transcribed with mouse mammary tumor virus reverse transcriptase (Life Technologies, Inc., Rockville, MD). 15-LOX-2 (351 bp) was amplified by the primer set S 5′-AACTCACCCCCACCACCATACACA-3′ and AS 5′-TTCCCGCCTCCATCTCCCAAAGT-3′ as previously described [6]. Primer pairs were used in RT-PCR analysis to detect PPAR-γ (γS 5′-TCTCTCCGTAATGGAAGACC-3′; γAS 5′-GCATTATGAGCATCCCCAC-3′; γ2S 5′-GCGATTCCTTCACTGCTAC-3′) [17] and 36B4 (S, 5′-CAGCTCTGGAGAACTGCTG-3′; AS 5′-GTGTACTCAGTCTCCACAGA-3′) [18]. The PCR products were electrophoretically separated, transferred onto a nylon membrane, and probed with 15-LOX-2 (5′-TCTACCAAGAACAGAGTCTC-3′), total γ (5′-GAGTACCAAAGTGCAATCAA-3′),

γ2-specific (5′-GTCTGCAAACATATCACA-3′), or 5′-GTGAGGTCACTGTGCCAG-3′ (36B4) ^{32}P radiolabelled oligonucleotide probes. RT-PCR cDNA products were subcloned using the TOPO TA system (Invitrogen, Carlsbad, CA), sequenced using an automated system (Seqwright, Houston, TX) and subjected to a BLAST analysis for sequence verification.

Western Blot Analysis

Whole cell lysates were prepared as previously described [16]. Specifically, 100 μg of protein was loaded in each lane, run on a 7.5% sodium dodecyl sulfate polyacrylamide gel electrophoresis gel, and transferred onto a nitrocellulose membrane (Schleicher and Schuell Bioscience, Keene, NH). The membrane was blocked overnight in Tris-buffered saline (TBS) solution and 0.1% Tween 20 containing 3.0% bovine serum albumin (BSA) and fraction V (United States Biological, Swampscott, MA). Rabbit primary antibodies, including anti-PPAR-γ (Santa Cruz Biotechnology, Inc.) or anti–15-LOX-2 (Oxford Biomedical Research, Inc.), were incubated overnight at 4°C. The appropriate HRP-conjugated secondary antibody (Pierce Chemical Co.) in TBS solution and 0.1% Tween 20 was used at 25°C for 1 to 2 hours. The signals were detected using the Super Signal chemiluminescence system (Pierce Chemical Co.).

Immunofluorescence Analysis of 15-LOX-2 Subcellular Distribution

All cells were grown on laminin-coated coverslips. Coverslips were fixed with 1% paraformaldehyde and permeabilized using 1% Triton X-100. Samples were then blocked with 3% fatty acid–free BSA solution in TBS containing 0.1% Tween 20 (TBST). Primary rabbit polyclonal antibody that recognizes 15-LOX-2 was diluted to 2.5 μg/ml in 3% BSA solution and incubated overnight at 4°C. Samples were rinsed twice with TBS and incubated with Alexa-488–conjugated goat antirabbit secondary antibody (Ex 495/Em 519; Molecular Probes) in a 3% BSA solution.

After the cells were stained with secondary antibodies, counterstaining was performed with 500 nM DAPI (4′,6-diamidino-2-phenylindole dilactate; Ex 358/Em 461; Molecular Probes) to identify the nuclei and with 1 U/ml Alexa-594 phalloidin (Ex 590/Em 617; Molecular Probes) to stain the cytoplasmic actin in 3% BSA solution containing TBST at 4°C. After overnight incubation, samples were washed three times in TBS, rinsed with distilled water, and mounted on glass slides using an antifade solution (Prolong; Molecular Probes). Slides were then analyzed by epifluorescence microscopy and data were acquired using digital image analysis, as previously described [16]. The controls consisted of secondary antibody alone or nonspecific primary antibody that were imaged using conditions that resolve the Alexa-488–conjugated goat antirabbit secondary antibody.

Determination of 15-S-HETE in Prostate Cells and Tissue Culture Medium

Various cell lines were plated in 100-mm tissue culture dishes to attain 70% to 75% confluence. Cells were then incubated with 10 μM AA for 30 minutes and 1 hour. The culture medium was collected at both time points, and cells were harvested at 1 hour by trypsinization and subjected to HETE extraction. Intracellular 15-*S*-HETE were extracted using the method of Kempen et al. [19] with modifications. Briefly, cells were resuspended in 500 μl of phosphate-buffered saline (PBS), and 20 μl of 1 N citric acid and 2.5 μl of 10% BHT were added to prevent free radical peroxidation. HETE was extracted with 2 ml of hexane/ethyl acetate (1:1, vol/vol) thrice. The upper organic phases were pooled and evaporated to dryness under a stream of nitrogen at room temperature. All extraction procedures were performed under conditions of minimal light. Samples were then reconstituted in 200 μl of methanol and 10 mM ammonium acetate buffer (70:30, vol/vol), pH 8.5, prior to analysis by LC/MS/MS.

15-*S*-HETE in the cell culture medium was extracted using a solid-phase method. An aliquot of 10 μl of 10% BHT was added to 1 ml of cell culture medium. The solution was applied to a Sep-Pak C18 cartridge (Waters Corporation, Milford, MA) that had been preconditioned with methanol and water. HETE were eluted with 1 ml of methanol. The eluate was evaporated under a stream of nitrogen and the residue was dissolved in 100 μl of methanol and 10 mM ammonium acetate buffer (70:30, vol/vol), pH 8.5.

LC/MS/MS

LC/MS/MS was performed using a tandem mass spectrometer (Micromass Quattro Ultima MS Technologies; Waters Corporation) equipped with an Agilent HP 1100 binary pump high-pressure liquid chromatography inlet. Eicosanoid metabolites were separated using a Luna 3-μm phenyl–hexyl 2 × 150 mm column (Phenomenex, Torrance, CA). The mobile phase consisted of 10 mM ammonium acetate, pH 8.5 (phase A), and methanol (phase B). The flow rate was 250 μl/min and the column temperature was maintained at 50°C. The sample injection volume was 25 μl. Samples were kept at 4°C during the analysis. 15-*S*-HETE was detected using electrospray negative ionization and multiple reaction monitoring of transitions at *m*/*z* 319.4→219.3. Fragmentation for the HETE was performed using argon as the collision gas at a collision cell pressure of 2.10×10^{-3} Torr. The results were expressed as nanograms of 15-*S*-HETE per 10^6 cells. The cell number was measured with an electronic particle counter (Coulter, Hialeah, FL).

In Situ Hybridization (ISH)

For the purpose of ISH, a 1059-bp fragment of 15-LOX-2 was amplified using the primer sets 5′-TGCCTCTCGCCATCCAGCT-3′ and 5′-TGTTCCCCTGGGATTTAGATGGA-3′ as previously described [6]. After being subcloned in sense and antisense orientations into Bluescript KS II vector, the 1059-bp sequence was verified and used for probe preparations in ISH. ISH on human tissue sections was performed according to the method of Xu et al. [20], with appropriate hybridization controls.

15-LOX-2 or PPAR-γ Forced Expression

Normal epithelial cell primary cultures (NHBE and HMEC) or epithelial tumor cells that had been selected for the highest level of PPAR-γ expression (PC-3, Calu I, MDA453, HaCaT, SW-620, U-9, and ASPC-1) were transiently cotransfected with 0.5, 1.0, or 2.0 μg of human PPAR-γ cDNA (provided by Dr. Alex Elbrecht) or 15-LOX-2 cDNA, respectively, using FuGENE 6 (DNA ratio, 3:1; Roche Diagnostic Corporation, Indianapolis, IN) overnight in serum-free medium (SFM). Cell cultures were then replated and used for experiments. After 2 days, transfected cells were placed in SFM and incubated either alone or with 1 or 10 μM 15-*S*-HETE (BIOMOL Research Laboratories, Inc., Plymouth Meeting, PA) for 14 to 16 hours. Protein extracts were made and analyzed for 15-LOX-2 or PPAR-γ expression by Western blot analysis.

Biotinylated-15-S-HETE Binding to PPAR-γ

PC-3 cells were used to examine the binding of biotinylated 15-*S*-HETE to endogenous PPAR-γ. Nuclear lysates were prepared by suspending cells in 400 μl of an ice-cold hypotonic buffer (containing 10 mM HEPES, pH 7.9, 1.5 mM $MgCl_2$, 10 mM KCl, 0.5 mM DTT, 100 μg/ml aprotinin, 5 μg/ml leupeptin, and 1 μg/ml pepstatin) and incubating on ice for 15 minutes. NP40 was added to a final concentration of 0.5% in 500 μl final volume. Next, the tubes were vortexed for 10 seconds and then centrifuged at 6500*g* for 10 minutes at 4°C. The supernatant was discarded and the nuclei were resuspended in 50 μl of a buffer containing 20 mM HEPES, pH 7.9, 25% glycerol, 420 mM NaCl, 1.5 mM $MgCl_2$, 0.2 mM EDTA, 0.5 mM DTT, 0.2 mM PMSF, 10 μg/ml aprotinin, 5 μg/ml leupeptin, and 1 μg/ml pepstatin. The tubes were incubated on ice for 20 minutes and then centrifuged for 10 minutes at 12,000*g* at 4°C. The resulting supernatant (nuclear extract) was then used for ligand binding studies.

Nuclear lysate (300 μg) was incubated with 5 or 10 μg of biotinylated 15-*S*-HETE in 225 μl of binding buffer containing 26 mM HEPES, pH 7.9, 26% glycerol, 120 mM KCl, 10 mM $MgCl_2$, 2 mM EDTA, 2 mM DTT, μg/ml aprotinin, 5 μg/ml leupeptin, and 1 μg/ml pepstatin for 30 minutes at 25°C. Control nuclear lysates that were pretreated with 10 μM of unlabeled 15-*S*-HETE for 10 minutes at 37°C were incubated with 10 μg of biotinylated 15-*S*-HETE in binding buffer for 30 minutes at 25°C. Biotinylated 15-*S*-HETE was bound to 25 μl of NeutrAvidin beads (Pierce Chemical Co.) by incubation at room temperature in binding buffer while mixing for 30 minutes. The agarose beads were then washed three times in PBS, resuspended in 20 to 30 μl of SDS-PAGE sample buffer, and boiled for 5 minutes. Samples were resolved by 7.5% PAGE, transferred to a nitrocellulose membrane, and blocked with 3% BSA overnight at 4°C. Western analysis using an anti-PPAR-γ monoclonal antibody (Santa Cruz Biotechnology, Inc.) was performed and detected as previously described [16].

To determine if binding of biotinylated-15-*S*-HETE was restricted to the *PPAR-γ* ligand binding domain (LBD), COS-1 cells were transfected with a chimeric expression plasmid containing the *PPAR-γ* LBD fused to a Gal4–DNA binding domain (DBD). Total cell lysates were prepared and subjected to affinity isolation using biotinylated 15-*S*-HETE as described above.

15-S-HETE–Mediated PPAR-γ Transactivation in PC3 Cells

To determine if extraneous 15-*S*-HETE could transactivate endogenous PPAR-γ, PC3 cells were transfected with either 1.5 μg of DR1 luciferase (LUC) [21] or acyl-CoA oxidase–peroxisome proliferator response element–thymidine kinase–LUC [(AOx-PPRE)3-TK-LUC] [22] reporter plasmids. Transfection efficiency was normalized using 500 ng of p-SVβ Gal expression plasmid (Promega, Inc. Madison, WI) as an internal control and the reporter assay analysis was performed as previously described [23]. LUC activity was expressed as relative LUC activity in fold increase after normalization to β-gal activity.

To determine if the binding of 15-*S*-HETE could transactivate PPAR-γ, transfection experiments performed using expression plasmids that contain either Gal4–DBD (amino acids 1–147) coupled to PPAR-γ LBD (amino acids 174–475) or fusion protein (or just Gal4–DBD as control) [24] were used to transfect PC 3 cells in six-well tissue culture plates. Either plasmid (1.0 μg) plus 1.0 μg of $(Gal4_{UAS})_4$–TK–LUC reporter plasmid [25] were cotransfected using Fugene 6, (Roche Diagnostics Corporation). PPAR-γ ligand, 15-*S*-HETE (5–10 μM) in ethanol, or ethanol alone was added 24 hours after the addition of DNA. LUC activity was measured 6 hours after adding the ligands.

Densitometry

All densitometric analyses were performed using a Personal Densitometer SI (Amersham Biosciences, Piscataway, NJ) and the corresponding software program, ImageQuant (Amersham Biosciences). Images were quantified using NIH Image J (National Institutes of Health). The density of the proteins analyzed was normalized to actin controls and represented graphically as a percentage of the transfection control.

Scoring of Stained Sections and RT-PCR or Western Gray Level Intensity

The sections stained by IHC or ISH for 15-LOX-2 were reviewed by light microscopy and scored as positive or negative, where positive staining indicates that 10% or more of the epithelial cells were immunopositive. RT-PCR and Western blot data were scored as 1 to 3+ based on their relative gray level intensity.

Statistical Analyses

A statistical analysis of stained sections was performed using the McNemar test to determine the association between the staining results in distant normal and cancerous tissues. The Kendall test is used to determine the accordance between ISH and IHC. *P* values were generated using Statistica version 4.1 for the PowerMac (StatSoft, Tulsa, OK). RT-PCR and Western gray level intensity or 15-*S*-HETE levels were analyzed statistically using the Statview software program (SAS Institute, Inc., Cary, NC). Student's

t tests were used to determine the significance ($P < .01$) between mean group values.

Results

Inverse Expression Between 15-LOX-2 and PPAR-γ in Normal and Malignant Epithelial Cells

Normal primary epithelial cell cultures derived from the prostate (PrEC), breast (HMEC), lung (NHBE), bladder (SVHUC), and skin (NK) all expressed mRNA and protein levels that were high for 15-LOX-2 (Figure 1) and low for PPAR-γ (Figure 2). In contrast, malignant and some transformed epithelial cells including those from the prostate (PC-3 and DU145), breast (MDA453), lung (Calu I), bladder (U-9 and U-14), skin (HaCaT), and pancreas (Mia PaCa-2 and ASPC-1) exhibited the inverse mRNA and protein expression pattern, namely, low 15-LOX-2 levels (Figure 1) and high PPAR-γ levels (Figure 2). The relative intensities of RNA and protein expression are summarized in Table 1. In other epithelial tumor cells, including prostate (LNCaP), lung (MSK-3), breast (MCF-7 and SK-BR-3), and skin (SCC-M7 and SCC-P9), we observed a similar trend of low 15-LOX-2 mRNA and protein expression (Figure 1, Table 1), but the levels of PPAR-γ, although present, were not as high as in other malignant cells (Figure 2, Table 1).

We previously reported that 15-LOX-2 mRNA and protein levels were high in normal EEC and low in esophageal cancer cells (TE-3 and TE-12) [26]. Results from the current study showed that PPAR-γ expression was high in TE-3 and TE-12 and low in EEC. In contrast, the levels of both 15-LOX-2 and PPAR-γ were mixed in colon cancer cells (HCT-115, SW-480, and SW620), depending on the tumor cell line (Table 1). Primary PrSt and PrSM cultures did not express 15-LOX-2 and expressed very low levels of PPAR-γ (Table 1). In neural crest–derived cells (normal human melanocytes and MeWo, 3S5, and 70W melanoma cells) or hepatic tumor cells (Hep G2 and Hep 3B), mRNA and protein levels of 15-LOX-2 and PPAR-γ were absent to low (Table 1, Figure 1). Northern blot analysis also confirmed the inverse mRNA expression pattern between 15-LOX-2

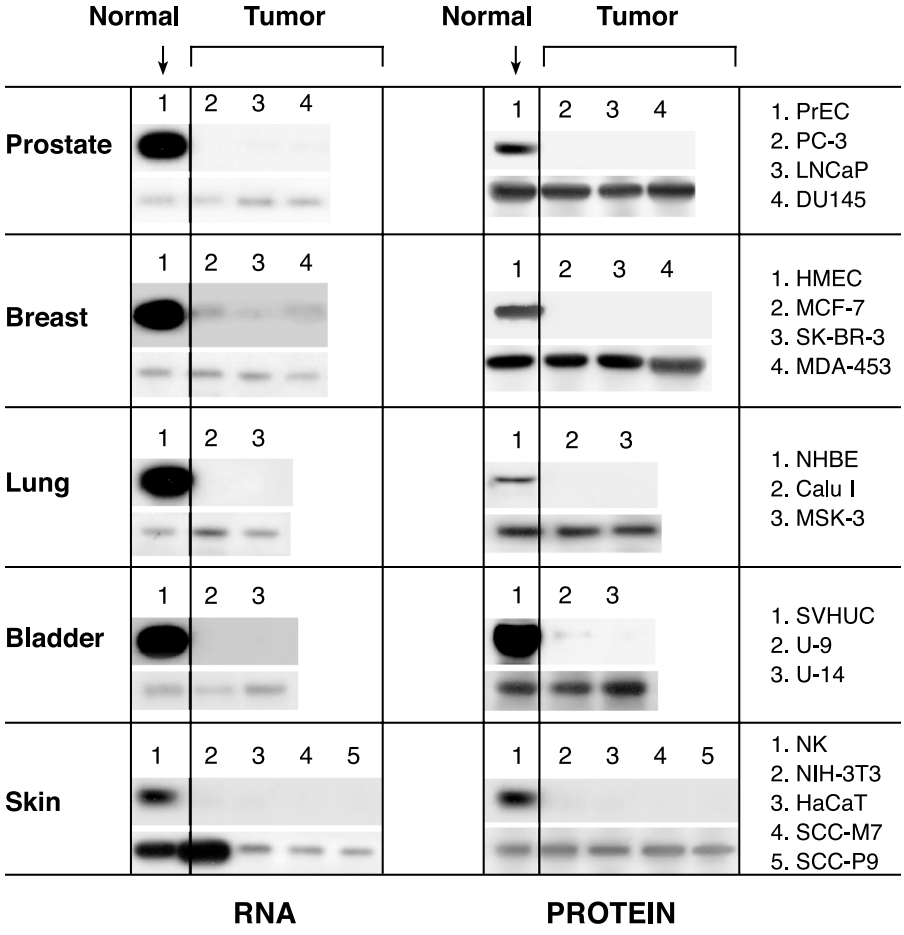

Figure 1. *15-LOX-2 expression is high in normal epithelial cells and low in tumor cells. High levels of 15-LOX-2 RNA were detected by RT-PCR in normal epithelial cells, including those from the prostate (PrEC), breast (HMEC), lung (NHBE), bladder (SVHUC), and skin (NK), at various cycle numbers (25, 30, 35, and 40). Trace levels of 15-LOX-2 RNA were detected in breast cancer cells (MCF-7, SK-BR-3, and MDA-453) and no 15-LOX-2 RNA was detected in the prostate (PC-3, LNCaP, and DU145), lung (Calu I and MSK-3), bladder (U-9 and U-14), or skin (NIH-3T3, HaCaT, SCC-M7, and SCC-P9) at any cycle number. Consistent with RT-PCR, high levels of 15-LOX-2 protein were detected in all normal epithelial cells. No 15-LOX-2 protein was detected in any tumor cells.*

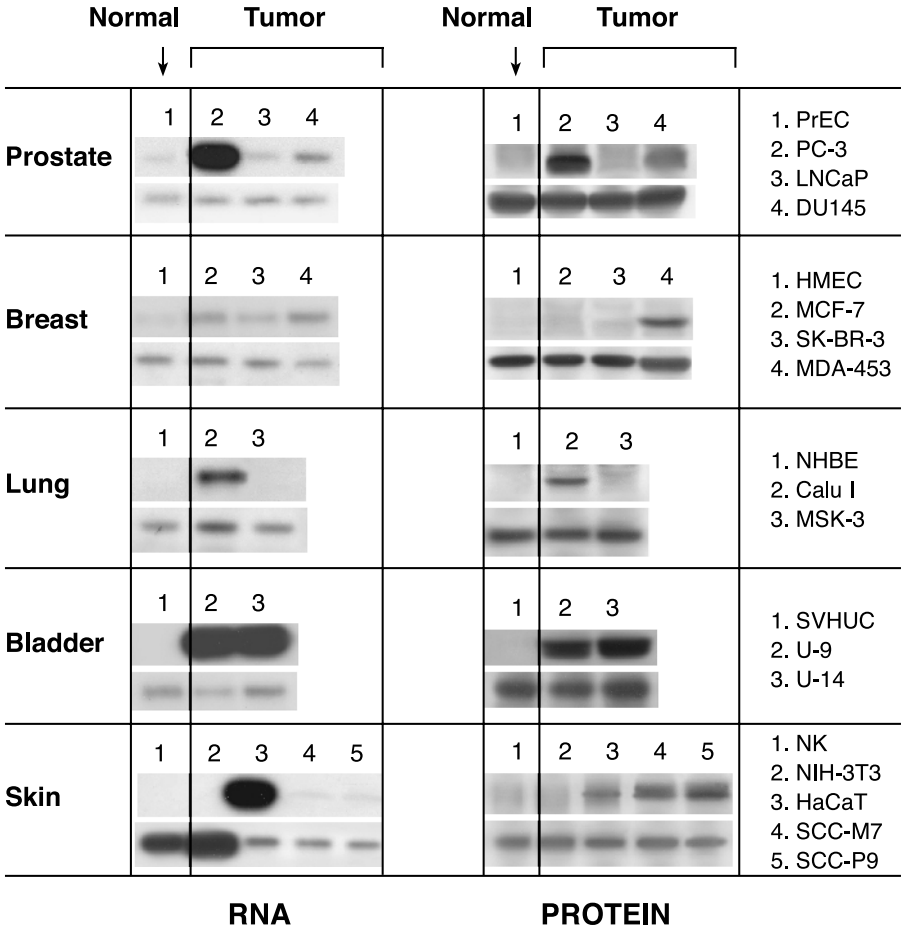

Figure 2. *PPAR-γ expression is high in tumor cells and low in normal epithelial cells. High levels of PPAR-γ RNA were detected by RT-PCR in nearly all cancer cells, including those from the prostate (PC-3 and DU145), breast (SK-BR-3), lung (Calu I), bladder (U-9 and U-14), and skin (HaCaT) and, to a lesser degree, in the prostate (LNCaP), breast (MCF-7 and MDA-453), lung (MSK-3), and skin (NIH-3T3, SCC-M7, and SCC-P9) at various cycle numbers (25, 30, 35, and 40). No PPAR-γ RNA was detected by RT-PCR in normal epithelial cells, including those from the prostate (PrEC), breast (HMEC), lung (NHBE) or bladder (SVHUC), and skin (NK) at any cycle number. Consistent with the results of RT-PCR, high levels of PPAR-γ protein were detected in nearly all tumor cells, but no PPAR-γ protein was detected in any of the normal epithelial cells.*

and PPAR-γ expression in normal *versus* tumor cells (data not shown). These data highlight the inverse relationship between normal and tumor epithelial cell expression patterns of 15-LOX-2 and PPAR-γ.

Subcellular Distribution of 15-LOX-2 in Normal and Tumor Cells

As shown in Figure 3, normal epithelial cells expressed high levels of 15-LOX-2 in the cytoplasm, which was absent from tumor cells. The cytoplasmic distribution in normal epithelial cells occurred in vesicles that resembled Golgi or endoplasmic reticulum (ER), and was heavily concentrated in perinuclear areas, typically at one pole of the nucleus. Counterstaining with DAPI, which labeled nuclear DNA, indicated that little or no 15-LOX-2 was present in the nucleus. Counterstaining with Alexa-594 phalloidin, which labeled cytoplasmic actin, showed that no 15-LOX-2 was associated with actin bundles.

15-LOX-2 Expression in Normal and Tumor Epithelia

ISH-identified 15-LOX-2 mRNA in epithelial tissues revealed trends of expression similar to those observed in cells. Normal prostate, breast, bladder, and skin tissues expressed high levels of 15-LOX-2 mRNA, but such levels were not observed in tumor tissues (Figure 4). Normal epithelia found in samples taken from the bladder (5/5), breast (5/5), pancreas (6/6), prostate (5/5), and skin (9/9) all expressed high levels of 15-LOX-2 mRNA. Fewer of the corresponding tumors expressed 15-LOX-2 mRNA, specifically bladder (3/7), breast (3/7), pancreas (4/6), prostate (3/6), skin (5/9) and lung (3/7).

15-S-HETE Levels in Normal and Tumor Cells

In general, 15-*S*-HETE levels produced by the various cells corresponded to the expression levels of 15-LOX-2: high in PrEC, HMEC, NHBE, and SVHUC normal cells but low in PC-3, MDA 453, Calu I, and U14 cancer cells

(Figure 5). Both cells and medium were assayed for the presence of 15-*S*-HETE. On average, most (95 ± 1%) of the 15-*S*-HETE produced was present in the medium. The SVHUC cells were the only samples in which the levels of 15-LOX-2 expression did not exactly correspond to the amount of 15-*S*-HETE produced. This may be due to the less efficient release of 15-*S*-HETE (88 ± 1%) from the SVHUC cells, which was significantly different from all of the other cell lines (*t*-test significance values ranged from $P < .01$ to $P < .03$ when other cells were compared with SVHUC cells).

Table 1. Summary of Results from RT-PCR and Western Analyses for 15-LOX-2 and PPAR-γ Gene Expression in Multiple Normal and Tumor Cell Lines*.

Tissue Type	Tissue	Cell Line	15-LOX-2		PPAR-γ	
			RNA	Protein	RNA	Protein
Epithelial	Prostate	PrEC (N)	+++	+++	–	–
		PC-3 (T)	–	–	+++	+++
		LNCaP (T)	–	–	±	±
		DU145 (T)	–	–	+	+
	Breast	HMEC (N)	+++	+++	–	–
		MCF-7 (T)	±	–	+	±
		SK-BR-3 (T)	–	–	+	±
		MDA-453 (T)	±	–	++	+++
	Lung	NHBE (N)	+++	+++	–	–
		Calu I (T)	–	–	+++	+++
		MSK-3 (T)	–	–	+	+
	Bladder	SVHUC (N)	+++	+++	±	–
		U-9 (T)	–	–	+++	+++
		U-14 (T)	–	–	+++	+++
	Skin	NK (N)	+++	+++	–	–
		HaCaT (T)	–	–	+++	++
		SCC-M7 (T)	–	–	±	++
		SCC-P9 (T)	–	–	±	++
	Esophageal	EEC (N)	+++	+++	–	–
		TE-3 (T)	–	–	++	++
		TE-12 (T)	–	–	++	++
	Pancreas	AsPC-1 (T)	–	–	++	+++
		Panc-1 (T)	–	±	++	++
		MIA PaCa-2 (T)	–	–	+++	++
	Colon	HCT-115 (T)	–	–	+	–
		SW-480 (T)	±	±	+	–
		SW-620 (T)	++	++	+++	+
Nonepithelial	Melanocytic	NHMC (N)	–	–	–	–
		MeWo (T)	++	++	+	±
		3S5 (T)	+	+	–	±
		70W (T)	–	–	+	±
	Fibroblast	NIH-3T3 (N)	–	–	–	–
	Prostate	PrSt (N)	–	–	±	–
		PrSM (N)	–	–	±	–
	Liver	Hep G2 (T)	+	+	±	±
		Hep 3B (T)	+	+	±	±

All of the normal epithelial cells exhibited RT-PCR or protein intensity scores of (+++) for 15-LOX-2 expression including those from the prostate (PrEC), breast (HMEC), lung (NHBE), bladder (SVHUC), skin (NK), and esophagus (EEC). In contrast, no tumor cells received any intensity scores greater than one except for colon (SW-620) and melanoma (MeWo) cells. Conversely, PPAR-γ RT-PCR or protein intensity scores were high in many tumor cells including those from the prostate (PC-3 and DU145), breast (MA-453), lung (Calu I), bladder (U-9 and U-14), skin (HaCaT, SCC-M7, and SCC-P9) or esophagus (TE-3 and TE-12), pancreas (ASPC-1, Panc-28, and Mia PaCa), colon (SW-620), and, to a lesser extent, in the prostate (LNCaP), breast (MCF-7 and MDA-453), lung (MSK-3) and skin (NIH-3T3, SCC-M7, and SCC-P9), colon (HCT-115 and SW-480), and liver (Hep G3 and Hep 3B). No normal epithelial cells expressed PPAR-γ. Other cells including normal human melanocytes (NHMC), melanoma (70W), fibroblasts (NIH-3T3), prostate stromal cells (PrSt), or prostate smooth muscle cells (PrSM) did not express significant levels of either 15-LOX-2 or PPAR-γ. RT-PCR and Western blot data were scored as (+), (++), or (+++) based on their relative gray scale intensity.
*N, normal cell lines; T, tumor cell lines.

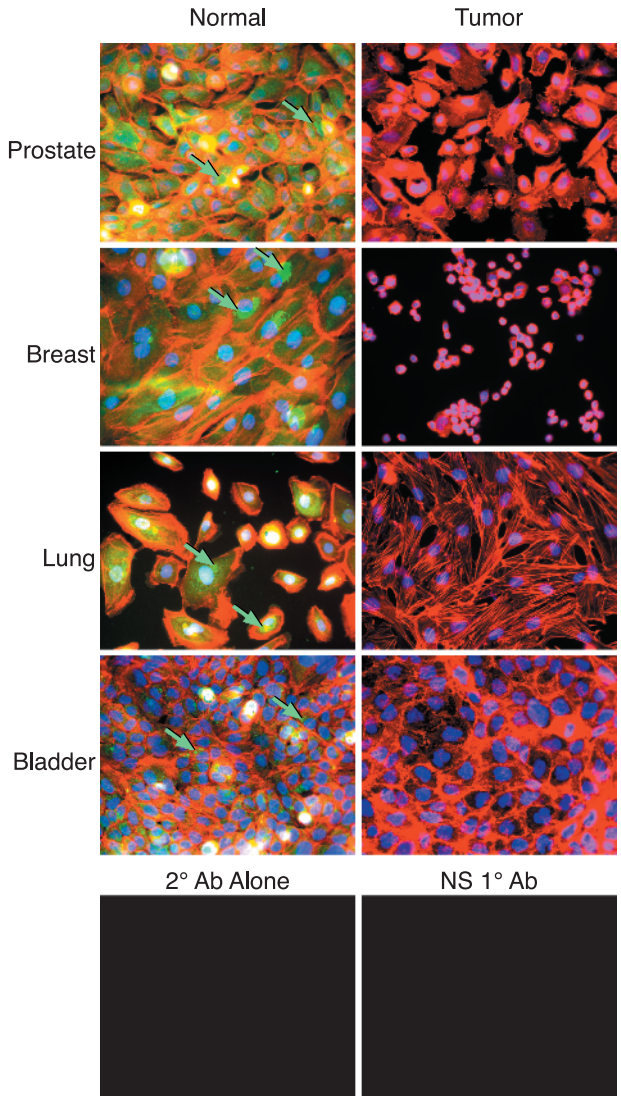

Figure 3. *Intracellular expression and distribution of 15-LOX-2. 15-LOX-2 expression was detected by immunofluorescence in normal epithelial cells, including those from the prostate (PrEC), breast (HMEC), lung (NHBE), or bladder (SVHUC). Intracellular 15-LOX-2 was located in vesicles or ER (arrows) and was heavily concentrated in perinuclear areas, typically at one nuclear pole. No 15-LOX-2 protein was detected in any of the tumor cells, including the prostate (PC-3), breast (MDA-453), lung (Calu I), and bladder (U-14). Controls consisted of secondary antibody alone or nonspecific primary antibody (bottom panels).*

15-S-HETE Binding to PPAR-γ in PC3 Cells

The direct binding of 15-*S*-HETE to PPAR-γ has yet to be demonstrated in cell nuclear lysates. Here we show that increasing concentrations (5 and 10 μg) of biotinylated-15-*S*-HETE bound increasing amounts of PPAR-γ protein. The specificity of this binding reaction was demonstrated by competition with unlabeled 15-*S*-HETE (Figure 6*A*). The involvement of the LBD in 15-*S*-HETE binding was demonstrated after transfecting COS-1 cells with chimeric protein containing the PPAR-γ LBD fused to a Gal4–DBD.

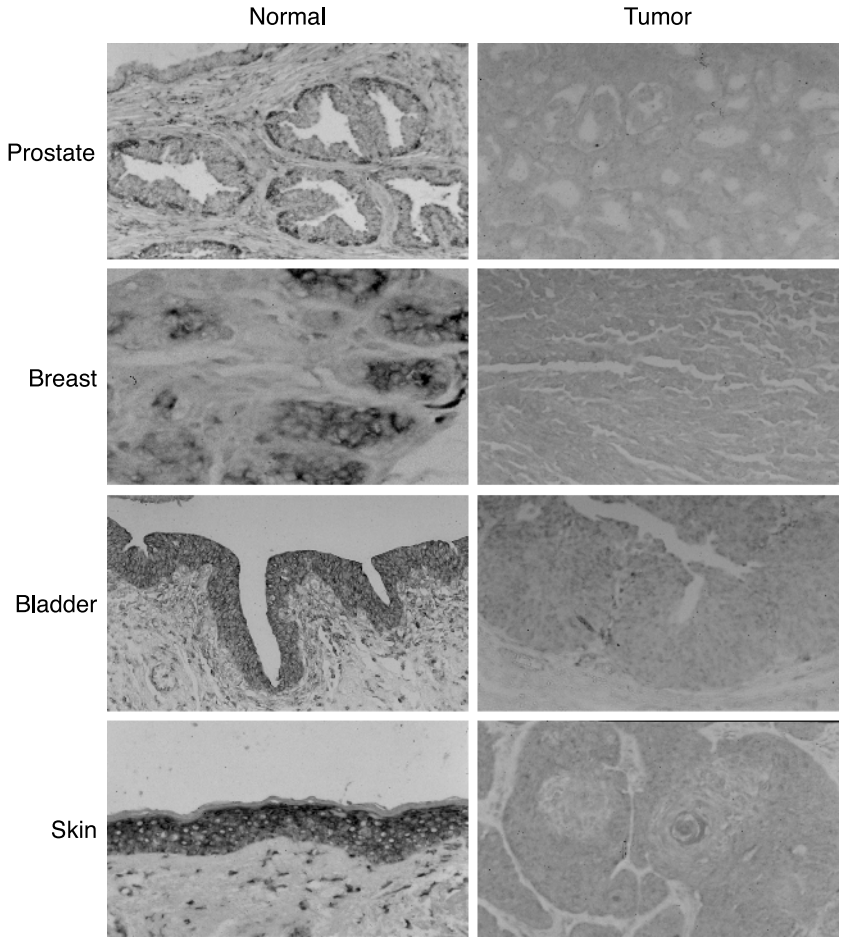

Figure 4. *ISH analysis of 15-LOX-2 expression in human tissue sections. Tumor and adjacent normal tissues were examined for 15-LOX-2 expression by ISH. Normal human prostate, bladder, skin, and breast normal tissues exhibited levels of 15-LOX-2 hybridization, whereas no signal was detected in the corresponding tumor tissues. Sections of formalin-fixed and paraffin-embedded human cancer tissues and distant normal tissues were hybridized with 15-LOX-2 antisense digoxigenin-labeled cRNA probe, which results in purple to blue staining of the positive signal in the cytoplasm. Original magnification, ×100.*

Biotinylated-15-*S*-HETE was used to affinity-isolate the PPAR-γ LBD–containing chimeric protein, which gave a similar protein isolation pattern as was observed for total PPAR-γ (data not shown).

15-S-HETE–Mediated Transactivation of PPAR-γ in PC3 Cells

The first enzyme of the peroxisomal β-oxidation pathway, AOx, contains upstream *cis*-acting regulatory regions termed PPREs, which are arranged as direct repeats [27]. When PC-3 cells were transfected with a DR-1 LUC construct followed by treatment with 15-*S*-HETE, there was nearly a two-fold induction of LUC reporter activity (Figure 6*B*). Similarly, another reporter construct containing three (AOx-PPRE)3-TK-LUC) was induced two-fold by 15-*S*-HETE treatment (Figure 6*C*).

15-S-HETE–Mediated Ligand Transactivation Is Specific for PPAR-γ LBD

To determine if PPAR-γ LBD is involved in 15-*S*-HETE transactivation, COS-1 cells were cotransfected with GAL4-DBD/mPPARγ LBD in combination with (GAL4) LUC reporter plasmid. (Figure 6*D*). Treatment of transfected cells with 5 or 10 μM 15-*S*-HETE caused a 3- and 12-fold increase in LUC activity, respectively, in comparison with ethanol-treated control samples.

Inverse Relationship between 15-LOX-2 and PPAR-γ in Normal Cells Compared with Tumor Cells

The inverse relationship between 15-LOX-2 and PPAR-γ expression in normal cells compared with tumor cells suggests that a feedback mechanism regulates the expression of these proteins. We further examined this relationship by overexpressing PPAR-γ in epithelial cells and 15-LOX-2 in tumor cells. We previously showed that overexpression of PPAR-γ1 and PPAR-γ2 each caused a dose-dependent downregulation of 15-LOX-2 protein expression in PrEC that was augmented by treatment with the 15-*S*-HETE ligand [28]. In the present study, we found that overexpression of PPAR-γ1 (Figure 7*A*) caused downregulation of 15-LOX-2 in normal epithelial cells from breast (HMEC) or lung (NHBE) tissues, which was enhanced by 15-*S*-HETE and, to a lesser extent, by AA—an effect that also occurred with PPAR-γ2 (data not shown).

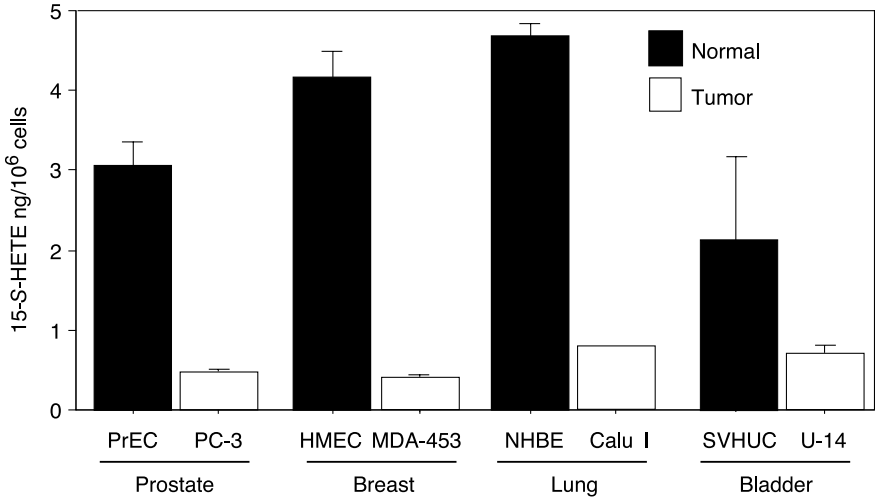

Figure 5. *15-S-HETE production in normal and tumor cells. To examine 15-S-HETE production, normal epithelial cells from the prostate (PrEC), breast (HMEC), lung (NHBE), or bladder (SVHUC) were paired with tumor cells from the prostate (PC-3), breast (SK-BR-3), lung (Calu I), and bladder (U-14) that expressed high levels of PPAR-γ. Preconfluent monolayers of cells in 100-mm tissue culture dishes were washed with serum-free medium, and fresh serum-free medium containing 10 μM arachidonic acid was added. After 30 and 60 minutes, cells and medium were processed for LC/MS/MS. 15-S-HETE detection was validated using a deuterated 15-S-HETE-d_8 internal standard. All values were normalized to a specific cell number of 1×10^6. Data shown are the mean ± SD from two experiments run in duplicate. 15-S-HETE, 15-S-hydroxyeicosatetraenoic acid.*

To test for feedback-driven regulation of PPAR-γ expression by 15-LOX-2, we overexpressed 15-LOX-2 in tumor cells that were derived from a variety of epithelia. Tumor cell lines selected were based on the highest level of PPAR-γ expression observed in our initial studies: PC-3, MDA-453, Calu I, U-14, and AsPC-1. In all cell lines examined, we observed concentration-dependent downregulation of PPAR-γ protein levels with increasing amounts of 15-LOX-2

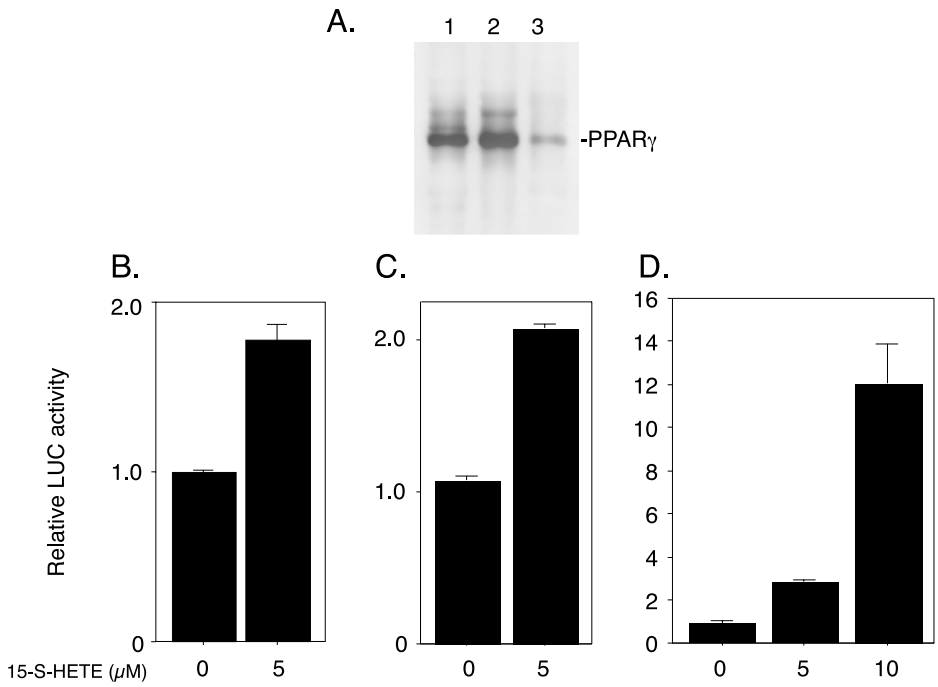

Figure 6. *15-S-HETE binding and transactivation of PPAR-γ. A. PPAR-γ from nuclear lysates that had bound biotinylated 15-S-HETE was isolated by affinity binding to streptavidin-coated agarose beads. Samples were separated by polyacrylamide gel electrophoresis and electrotransferred to nitrocellulose, and then PPAR-γ was detected by chemiluminescence using a mouse monoclonal antibody. As the concentration of biotinylated 15-S-HETE was increased from 5 μg (lane 1) to 10 μg (lane 2), there was more PPAR-γ protein bound to the beads. Unlabeled 15-S-HETE (10 μM) competed for the interaction of biotinylated 15-S-HETE (10 μg) with PPAR-γ protein (lane 3). PC-3 cells were transfected with (B) DR-1-LUC or (C) (AOx-PPRE)3-TK-LUC plasmid followed by treatment with 5 μM 15-S-HETE, which induced nearly a two-fold increase in LUC reporter activity using the (B) DR-1-LUC ($P < .001$) or a two-fold increase in LUC reporter activity using the (C) (AOx-PPRE)3-TK-LUC ($P < .001$). (D) LBD activity was measured after cotransfecting PC-3 cells with 1.0 μg of a chimeric expression vector pCMX-Gal-L-mPPARγ with 1.0 μg of TK-MH100x4-LUC reporter followed by treatment with 15-S-HETE. The PPAR-γ LBD was transactivated more than two-fold with 5 μM 15-S-HETE ($P < .001$) or approximately 10-fold with 10 μM 15-S-HETE ($P < .001$) as measured by LUC reporter activity.*

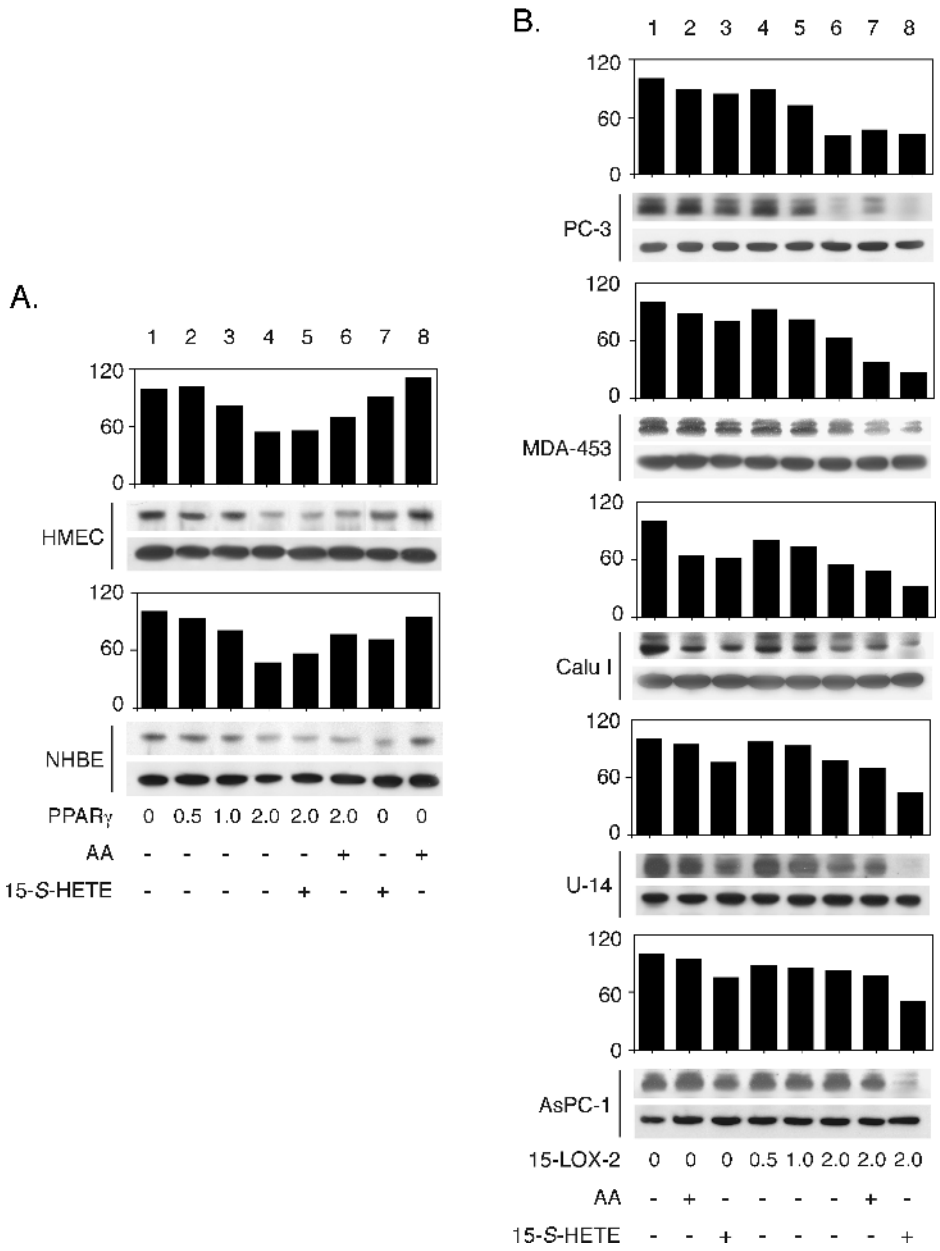

Figure 7. *Inverse effects caused by 15-LOX-2 (top panel) and PPAR-γ (bottom panel) expression in normal cells compared with cancer cells. (A) The forced expression of PPAR-γ in normal epithelial cells from the breast (HMEC) or lung (NHBE) suppressed the expression of 15-LOX-2—an effect that was enhanced by the addition of 15-S-HETE and, to a lesser extent, by AA. (B) The forced expression of 15-LOX-2 decreased the level of PPAR-γ in selected tumor cells, including those from the prostate (PC-3), breast (MDA-453), lung (Calu I), bladder (U-14), and pancreas (ASPC-1)—an effect that was enhanced by the addition of 15-S-HETE and, to a lesser extent, by AA. Densitometry was performed to determine the mean pixel density of each protein band. These values were first normalized to actin and then represented graphically as a percentage of the control band in lane 1. PPAR-γ, peroxisome proliferator–activated receptor γ; AA, arachidonic acid; 15-S-HETE, 15-S-hydroxyeicosatetraenoic acid; 15-LOX-2, 15-lipoxygenase-2.*

plasmid, a downregulation effect that was amplified by coincubation with 15-*S*-HETE (Figure 7*B*).

Discussion

Epithelial tissues give rise to a large number of cancers; however, it is generally difficult to find molecular determinants that are commonly regulated among the majority of epithelial cancers. Similarly, many epithelial tissues typically secrete unique molecular products, but few secretory products are commonly altered in a large variety of epithelial cancers. Our current study suggests that 15-LOX-2 and its enzymatic product, 15-*S*-HETE, or its receptor, PPAR-γ, comprise one set of candidate molecular determinants that changes in most normal *versus* malignant epithelial tissues.

In the original cloning report on human 15-LOX-2, Brash et al. [6] examined a number of tissues for mRNA expression by Northern blot analysis. They showed that certain epithelia containing tissues including prostate, lung, and

corneal tissues expressed 15-LOX-2, which was confirmed by RT-PCR in another study [29]. Our current study extended the analysis of 15-LOX-2 and PPAR-γ in epithelial tissues to other tissues, including the bladder, breast, colon, esophagus, lung, pancreas, and skin, and some of non-epithelial origin. We showed through systematic analysis that most epithelial tissues exhibit an inverse relationship between 15-LOX-2, its product 15-*S*-HETE, and PPAR-γ in normal *versus* tumor cells, and that this relationship may be regulated by a feedback mechanism. Because the PPAR-γ ligand, 15-*S*-HETE, is largely secreted as a free ligand based on our current studies, this may influence any potential feedback relationship between these molecules.

The secretory properties of 15-*S*-HETE have been known for some time, but their relationship to carcinogenesis is unclear. The production of 15-*S*-HETE as a part of mucin release was first described by Marom et al. [30] using human cultured airway cells in 1983. The release of 15-*S*-HETE was subsequently shown during allergic and asthmatic reactions [31–33], which may affect mast cell activity [34] or neutrophil function [35]. The release of 15-*S*-HETE can either increase or decrease the chemotaxis of inflammatory cells depending on the conditions and cells studied [36–39]. Our current observations revealed the localization of 15-LOX-2 with structures resembling ER or Golgi in all normal epithelial cells, but these structures were less apparent in virally transformed cells (Figure 3). Our current study also showed that 95 ± 1% of the 15-*S*-HETE was released into the growth medium by all normal epithelial cells examined, but that viral transformation decreased the efficiency of 15-*S*-HETE release. ER and Golgi are known to be associated with the synthesis, packaging, and release of secretory lipids and proteins [40–42]. Furthermore, SV40 transformation was shown to affect intracellular lipid transport into the Golgi apparatus [43]. The importance of 15-*S*-HETE release from epithelial cells and its relationship to the growth and development of epithelial cancer remain unknown. Further study is needed to determine whether the release of 15-*S*-HETE is involved in the homeostasis of normal epithelium, helps with immune surveillance, or has a paracrine influence on cancer cells that express PPAR-γ.

ISH analysis of normal and tumor samples revealed that *15-LOX-2* gene expression was primarily restricted to epithelial cells in normal tissues, but was reduced or lost in tumor tissues (Figure 4). These results are similar to the 15-LOX-2 expression patterns described in benign and malignant human prostate cancers [12]. In breast cancer, two of two cases of ductal carcinoma *in situ* (DCIS; data not shown) and four of seven cases of invasive carcinoma exhibited loss of 15-LOX-2 expression. Our data are consistent with RT-PCR data reported by Jiang et al. [44] on patient samples that examined normal DCIS and tumor tissues for 15-LOX-2 expression. Jiang et al. [44] also reported high levels of 15-LOX-2 mRNA in certain breast cancer cell lines including MCF-7, MDA MB231, and MRC-5, which contrasted with our findings of low levels of 15-LOX-2 mRNA in MCF-7, SK-BR-3, and MDA-453 cells using a different set of primers. Jiang et al. [44], however, did not examine protein levels in these cells, whereas we did not see protein produced in any of these cancer cell lines even though low levels of 15-LOX-2 mRNA are present. When taken together, these findings suggest that the loss of *15-LOX-2* gene expression may be regulated not only at the transcriptional level but also at the translational level.

Numerous reports have described the potential involvement of 15-*S*-HETE in asthmatic reactions [45–48]. Little, however, is known about the role of 15-LOX-2 in the development of lung cancer. Moody et al. [49] showed that LOX inhibitors can inhibit the growth of non small cell lung cancer cells in tissue culture and mouse xenografts. In contrast, 15-*S*-HETE production in A549 human lung adenocarcinoma cells significantly suppressed proliferation [50]. In our studies on lungs, all normal samples expressed the *15-LOX-2* gene, whereas four of seven cases did not express the *15-LOX-2* gene, which is consistent with our cell line data whereby normal NHBE expressed high levels of *15-LOX-2* gene and 15-*S*-HETE, which was lost in Calu I and MSK-3 lung cancer cells.

Although 15-LOX-2 was originally cloned from human hair rootlet cells, little is known about its role in skin cancer. Shappell et al. [51] examined both RNA and protein expression in benign and neoplastic sebaceous glands and other cutaneous adnexa. They observed that the strongest 15-LOX-2 expression is in the androgen-regulated secretory cells of sebaceous, apocrine, and eccrine glands, which decreased in skin-derived sebaceous neoplasms [51]. Our ISH studies were consistent with this report; all normal samples expressed the *15-LOX-2* gene but four of nine squamous cell carcinoma cases did not express the gene. Similarly, NK cells expressed high levels of 15-LOX-2 when compared to HaCaT, SCC-M7, or SCC-M9 cells.

Our ISH analysis of bladder or pancreatic tissues also revealed that 15-LOX-2 expression was either reduced or lost during tumor progression. In the bladder where all normal samples expressed the *15-LOX-2* gene, four of seven tumor cases did not express the gene. In the pancreas, where all normal samples expressed the *15-LOX-2* gene, two of six cases did not express the gene. No other studies on *15-LOX-2* gene expression in bladder have been reported. One study did not find 15-LOX-2 by RT-PCR in pancreas [29]. In the pancreas, however, the effects of antidiabetic thiazolidinediones on PPAR-γ function are well documented [52–54]. Overall, our ISH analysis of different cancer tissues also revealed that 15-LOX-2 expression was reduced or lost, consistent with RT-PCR analysis of cancer cell lines. Thus, loss of 15-LOX-2 during cancer progression might be a generalized phenomenon in most epithelial cancers.

PPAR-γ is activated by a number of polyunsaturated fatty acids and their derivatives [55], antidiabetic thiazolidinediones [56–60], 15 deoxy-Δ prostaglandin J_2 [24,61–63], and metabolites of the LOX pathway [8,10,64,65]. 15-*S*-HETE, a metabolite of *15-LOX-2* gene, was shown to activate the nuclear transcription factor PPAR-γ in macrophages and PC-3 cells [8,10]. Wigren et al. [66] also demonstrated that 5 μM 15-*S*-HETE caused a 12-fold

increase in activation of the LBD of PPAR-γ using a chimeric GAL4-DBD/mPPARγ LBD receptor in combination with a (GAL4)UAS4 E1b LUC reporter plasmid in RAW 264.7 murine macrophages and CV-1 monkey kidney cells. Similarly, the 15-LOX-1 gene product, 13-*S*-HODE, has been shown to activate PPAR-γ in colon tissue by increasing mitogen-activated protein kinase signaling, phosphorylation of the receptor, and thus downregulation of PPAR-γ activity [67]. The production of 13-*S*-HODE by 15-LOX-1 in colon cancer cells also downregulates PPARδ activity [68]. In addition, 13-*S*-HODE induces apoptosis in a colon tumor cell line treated with sodium butyrate by upregulation of 15-LOX-1 [69–71]. Prostate cancer cells also synthesize 13-*S*-HODE from LA [72] and respond to 15-*S*-HETE by activating PPAR-γ and inhibiting cellular proliferation [8].

Our current data are the first to show a direct interaction between 15-*S*-HETE and PPAR-γ by using biotinylated-15-*S*-HETE to affinity-isolate total PPAR-γ from PC-3 cell nuclear lysates (Figure 6*A*). Using the same biotinylated 15-*S*-HETE ligand binding method, we also observed that this interaction occurs with the LBD of PPAR-γ when we overexpressed chimeric GAL4-DBD/mPPAR LBD protein in COS-1 cells (data not shown). In these studies, unlabeled 15-*S*-HETE competing for biotinylated-15-*S*-HETE interaction with chimeric GAL4-DBD/mPPAR LBD protein was affinity-isolated from COS-1 total cell lysates (Figure 6*B*). The present study also shows that 15-*S*-HETE is able to transactivate PPAR-γ in three different reporter systems. The DR-1 and the (AOx-PPRE)3-TK-LUC reporters (Figure 6, *B* and *C*) were activated approximately two-fold by 5 μM 15-*S*-HETE, which is consistent with previous reports showing approximately a two-fold increase in LUC activity using 10 μM 15-*S*-HETE in PC-3 cells [8]. The present study also shows approximately a 12-fold increase in PPAR-γ LBD–driven LUC activity following stimulation with 10 μM 15-*S*-HETE, but only three-fold increase with 5 μM 15-*S*-HETE when using a chimeric GAL4-DBD/mPPARγ LBD LUC reporter system (Figure 6*D*). These data are similar to those observed by Wigren et al. [66] in RAW 264.7 murine macrophages using 5 μM 15-*S*-HETE with the same system. The differences between these studies are likely due to cell background, transfection efficiency, or possibly 15-*S*-HETE stability.

The relative contribution of each LOX, its products, the preference of substrates, and the extent of PPAR-γ activation and downstream targets may lead to differential responses in a given cell. Natural and synthetic agonists can cause growth inhibition, differentiation, and apoptosis in numerous tumor cell lines, according to cell type [73], suggesting the involvement of different pathways and genes. The present study demonstrated that the forced expression of 15-LOX-2 suppresses PPAR-γ in many types of epithelial cancer cells, which was augmented by treatment with 15-*S*-HETE. The mechanisms responsible for this suppressive feedback will require additional study; however, one factor that appears to promote this behavior is high levels of PPAR-γ. In the case of 15-LOX-2, in contrast, previous studies, the existence of multiple splice variants and transcriptional repression of 15-LOX-2 in the absence of methylation [13], as well as our data suggest that there are multiple regulation levels of this protein. As we previously shown, the overexpression of PPAR-γ alone or in combination with 15-*S*-HETE ligand downregulated 15-LOX-2 protein expression in PrEC [28]. In the current study, the suppression of 15-LOX-2 protein expression by PPAR-γ and 15-*S*-HETE was observed in HMEC and NHBE. Further studies are needed to determine if this occurs at the 15-LOX-2 promoter level.

In summary, our results identified 15-LOX-2 expression in a variety of human cells and tissues. All epithelial tumor tissues we studied displayed reduced 15-LOX-2 expression and 15-*S*-HETE production but increased PPAR-γ expression, compared with those in normal tissues. PPAR-γ transactivation analysis using 15-*S*-HETE indicated that this metabolite is a ligand in multiple epithelial tissues (data not shown). Furthermore, the inverse relationship between the inhibition of 15-LOX-2 expression by PPAR-γ in normal cells and the inhibition of PPAR-γ expression by 15-LOX-2 in tumor cells suggests that a feedback inhibition mechanism is involved in balancing the expression of these two proteins, which is amplified by the 15-*S*-HETE ligand. Based on these data, the loss of 15-LOX-2 expression may be a useful biomarker for the early identification of multiple epithelial cancer types.

Acknowledgements

We thank A. Elbrecht (Merck Research Laboratories, Rahway, NJ) for providing PPAR-γ expression plasmids; R. Evans (The Salk Institute for Biological Studies, La Jolla, CA) for providing the pCMX-Gal-L-mPPARγ and TK-MH100X4-LUC plasmids; C. K. Glass (University of California, San Diego, CA) for providing (AOx-PPRE)3-TK-LUC reporter plasmid; and E. M. McDonald (Department of Scientific Publications at M. D. Anderson Cancer Center, Houston, TX) for editorial expertise.

References

[1] Gillmor SA, Villasenor A, Fletterick R, Sigal E, and Browner MF (1997). The structure of mammalian 15-lipoxygenase reveals similarity to the lipases and the determinants of substrate specificity. *Nat Struct Biol* **4,** 1003–1009.

[2] Prigge ST, Boyington JC, Faig M, Doctor KS, Gaffney BJ, and Amzel LM (1997). Structure and mechanism of lipoxygenases. *Biochimie* **79,** 629–636.

[3] Brash AR (1999). Lipoxygenases: occurrence, functions, catalysis, and acquisition of substrate. *J Biol Chem* **274,** 23679–23682.

[4] Jisaka M, Kim RB, Boeglin WE, and Brash AR (2000). Identification of amino acid determinants of the positional specificity of mouse 8*S*-lipoxygenase and human 15*S*-lipoxygenase-2. *J Biol Chem* **275,** 1287–1293.

[5] Sigal E, Craik CS, Dixon RA, and Nadel JA (1989). Cloning and expression of human arachidonate 15-lipoxygenase. *Trans Assoc Am Physicians* **102,** 176–184.

[6] Brash AR, Boeglin WE, and Chang MS (1997). Discovery of a second 15*S*-lipoxygenase in humans. *Proc Natl Acad Sci USA* **94,** 6148–6152.

[7] Kuhn H, Barnett J, Grunberger D, Baecker P, Chow J, Nguyen B, Bursztyn-Pettegrew H, Chan H, and Sigal E (1993). Overexpression, purification and characterization of human recombinant 15-lipoxygenase. *Biochim Biophys Acta* **1169,** 80–89.

[8] Shappell SB, Gupta RA, Manning S, Whitehead R, Boeglin WE, Schneider C, Case T, Price J, Jack GS, Wheeler TM, et al. (2001).

15*S*-Hydroxyeicosatetraenoic acid activates peroxisome proliferator–activated receptor gamma and inhibits proliferation in PC3 prostate carcinoma cells. *Cancer Res* **61,** 497–503.

[9] Ricote M, Welch JS, and Glass CK (2000). Regulation of macrophage gene expression by the peroxisome proliferator–activated receptor-gamma. *Horm Res* **54,** 275–280.

[10] Huang JT, Welch JS, Ricote M, Binder CJ, Willson TM, Kelly C, Witztum JL, Funk CD, Conrad D, and Glass CK (1999). Interleukin-4–dependent production of PPAR-gamma ligands in macrophages by 12/15-lipoxygenase. *Nature* **400,** 378–382.

[11] Nagy L, Tontonoz P, Alvarez JG, Chen H, and Evans RM (1998). Oxidized LDL regulates macrophage gene expression through ligand activation of PPARgamma. *Cell* **93,** 229–240.

[12] Shappell SB, Boeglin WE, Olson SJ, Kasper S, and Brash AR (1999). 15-Lipoxygenase-2 (15-LOX-2) is expressed in benign prostatic epithelium and reduced in prostate adenocarcinoma. *Am J Pathol* **155,** 235–245.

[13] Tang S, Bhatia B, Maldonado CJ, Yang P, Newman RA, Liu J, Chandra J, Traag J, Klein RD, Fischer SM, et al. (2002). Evidence that arachidonate 15-lipoxygenase 2 is a negative cell cycle regulator in normal prostate epithelial cells. *J Biol Chem* **277,** 16189–16201.

[14] Bhatia B, Maldonado CJ, Tang S, Chandra D, Klein RD, Chopra D, Shappell SB, Yang P, Newman RA, and Tang DG (2003). Subcellular localization and tumor-suppressive functions of 15-lipoxygenase 2 (15-LOX-2) and its splice variants. *J Biol Chem* **278,** 25091–25100.

[15] Jack GS, Brash AR, Olson SJ, Manning S, Coffey CS, Smith JA Jr, and Shappell SB (2000). Reduced 15-lipoxygenase-2 immunostaining in prostate adenocarcinoma: correlation with grade and expression in high-grade prostatic intraepithelial neoplasia. *Hum Pathol* **31,** 1146–1154.

[16] Subbarayan V, Sabichi AL, Llansa N, Lippman SM, and Menter DG (2001). Differential expression of cyclooxygenase-2 and its regulation by tumor necrosis factor-alpha in normal and malignant prostate cells. *Cancer Res* **61,** 2720–2726.

[17] Fajas L, Auboeuf D, Raspe E, Schoonjans K, Lefebvre AM, Saladin R, Najib J, Laville M, Fruchart JC, Deeb S, et al. (1997). The organization, promoter analysis, and expression of the human *PPARgamma* gene. *J Biol Chem* **272,** 18779–18789.

[18] Laborda J (1991). 36B4 cDNA used as an estradiol-independent mRNA control is the cDNA for human acidic ribosomal phosphoprotein PO. *Nucleic Acids Res* **19,** 3998.

[19] Kempen EC, Yang P, Felix E, Madden T, and Newman RA (2001). Simultaneous quantification of arachidonic acid metabolites in cultured tumor cells using high-performance liquid chromatography/electrospray ionization tandem mass spectrometry. *Anal Biochem* **297,** 183–190.

[20] Xu XC, Ro JY, Lee JS, Shin DM, Hong WK, and Lotan R (1994). Differential expression of nuclear retinoid receptors in normal, premalignant, and malignant head and neck tissues. *Cancer Res* **54,** 3580–3587.

[21] Tontonoz P, Hu E, Graves RA, Budavari AI, and Spiegelman BM (1994). mPPAR gamma 2: tissue-specific regulator of an adipocyte enhancer. *Genes Dev* **8,** 1224–1234.

[22] Ricote M, Huang J, Fajas L, Li A, Welch J, Najib J, Witztum JL, Auwerx W, Palinski W, and Glass CK (1998). Expression of the peroxisome proliferator–activated receptor gamma (PPARgamma) in human atherosclerosis and regulation in macrophages by colony stimulating factors and oxidized low density lipoprotein. *Proc Natl Acad Sci USA* **95,** 7614–7619.

[23] Salas TR, Reddy SA, Clifford JL, Davis RJ, Kikuchi A, Lippman SM, and Menter DG (2003). Alleviating the suppression of glycogen synthase kinase-3beta by Akt leads to the phosphorylation of cAMP-response element-binding protein and its transactivation in intact cell nuclei. *J Biol Chem* **278,** 41338–41346.

[24] Forman BM, Tontonoz P, Chen J, Brun RP, Spiegelman BM, and Evans RM (1995). 15-Deoxy-delta 12, 14-prostaglandin J2 is a ligand for the adipocyte determination factor PPAR gamma. *Cell* **83,** 803–812.

[25] DiRenzo J, Soderstrom M, Kurokawa R, Ogliastro MH, Ricote M, Ingrey S, Horlein A, Rosenfeld MG, and Glass CK (1997). Peroxisome proliferator–activated receptors and retinoic acid receptors differentially control the interactions of retinoid X receptor heterodimers with ligands, coactivators, and corepressors. *Mol Cell Biol* **17,** 2166–2176.

[26] Xu XC, Shappell SB, Liang Z, Song S, Menter D, Subbarayan V, Iyengar S, Tang DG, and Lippman SM (2003). Reduced 15*S*-lipoxygenase-2 expression in esophageal cancer specimens and cells and upregulation *in vitro* by the cyclooxygenase-2 inhibitor, NS398. *Neoplasia* **5,** 121–127.

[27] Tugwood JD, Issemann I, Anderson RG, Bundell KR, McPheat WL, and Green S (1992). The mouse peroxisome proliferator activated receptor recognizes a response element in the 5′ flanking sequence of the rat acyl CoA oxidase gene. *EMBO J* **11,** 433–439.

[28] Subbarayan V, Sabichi AL, Kim J, Llansa N, Logothetis CJ, Lippman SM, and Menter DG (2004). Differential PPAR-γ isoform expression and agonist effects in normal and malignant prostate cells. *Cancer Epidemiol Biomark Prev* in press.

[29] Krieg P, Marks F, and Furstenberger G (2001). A gene cluster encoding human epidermis–type lipoxygenases at chromosome 17p13.1: cloning, physical mapping, and expression. *Genomics* **73,** 323–330.

[30] Marom Z, Shelhamer JH, Sun F, and Kaliner M (1983). Human airway monohydroxyeicosatetraenoic acid generation and mucus release. *J Clin Invest* **72,** 122–127.

[31] Henke D, Danilowicz RM, Curtis JF, Boucher RC, and Eling TE (1988). Metabolism of arachidonic acid by human nasal and bronchial epithelial cells. *Arch Biochem Biophys* **267,** 426–436.

[32] Mattoli S, Mezzetti M, Fasoli A, Patalano F, and Allegra L (1990). Nedocromil sodium prevents the release of 15-hydroxyeicosatetraenoic acid from human bronchial epithelial cells exposed to toluene diisocyanate *in vitro*. *Int Arch Allergy Appl Immunol* **92,** 16–22.

[33] Vignola AM, Chanez P, Campbell AM, Bousquet J, Michel FB, and Godard P (1993). Functional and phenotypic characteristics of bronchial epithelial cells obtained by brushing from asthmatic and normal subjects. *Allergy* **48,** 32–38 discussion 39–48.

[34] Lazarus SC (1987). The role of mast cell–derived mediators in airway function. *Am Rev Respir Dis* **135,** S35–S38.

[35] Hafstrom I, Ringertz B, Palmblad J, and Malmsten C (1984). Effects of auranofin on leukotriene production and leukotriene stimulated neutrophil function. *Agents Actions* **15,** 551–555.

[36] Johnson HG, McNee ML, and Sun FF (1985). 15-Hydroxyeicosatetraenoic acid is a potent inflammatory mediator and agonist of canine tracheal mucus secretion. *Am Rev Respir Dis* **131,** 917–922.

[37] Jeffrey P and Zhu J (2002). Mucin-producing elements and inflammatory cells. *Novartis Found Symp* **248,** 51–68 discussion 68–75, 277–282.

[38] Profita M, Sala A, Siena L, Henson PM, Murphy RC, Paterno A, Bonanno A, Riccobono L, Mirabella A, Bonsignore G, et al. (2002). Leukotriene B4 production in human mononuclear phagocytes is modulated by interleukin-4–induced 15-lipoxygenase. *J Pharmacol Exp Ther* **300,** 868–875.

[39] Ternowitz T, Fogh K, and Kragballe K (1988). 15-Hydroxyeicosatetraenoic acid (15-HETE) specifically inhibits LTB4-induced chemotaxis of human neutrophils. *Skin Pharmacol* **1,** 93–99.

[40] Blazquez M and Shennan KI (2000). Basic mechanisms of secretion: sorting into the regulated secretory pathway. *Biochem Cell Biol* **78,** 181–191.

[41] Bankaitis VA and Morris AJ (2003). Lipids and the exocytotic machinery of eukaryotic cells. *Curr Opin Cell Biol* **15,** 389–395.

[42] Holthuis JC, van Meer G, and Huitema K (2003). Lipid microdomains, lipid translocation and the organization of intracellular membrane transport. *Mol Membr Biol* **20,** 231–241(Review).

[43] Sleight RG and Abanto MN (1989). Differences in intracellular transport of a fluorescent phosphatidylcholine analog in established cell lines. *J Cell Sci* **93** (Part 2), 363–374.

[44] Jiang WG, Douglas-Jones A, and Mansel RE (2003). Levels of expression of lipoxygenases and cyclooxygenase-2 in human breast cancer. *Prostaglandins Leukot Essent Fat Acids* **69,** 275–281.

[45] Chu HW, Balzar S, Westcott JY, Trudeau JB, Sun Y, Conrad DJ, and Wenzel SE (2002). Expression and activation of 15-lipoxygenase pathway in severe asthma: relationship to eosinophilic phenotype and collagen deposition. *Clin Exp Allergy* **32,** 1558–1565.

[46] Bradding P, Redington AE, Djukanovic R, Conrad DJ, and Holgate ST (1995). 15-Lipoxygenase immunoreactivity in normal and in asthmatic airways. *Am J Respir Crit Care Med* **151,** 1201–1204.

[47] Nasser SM and Lee TH (2002). Products of 15-lipoxygenase: are they important in asthma? *Clin Exp Allergy* **32,** 1540–1542.

[48] Kumlin M, Ohlson E, Bjorck T, Hamberg M, Granstrom E, Dahlen B, Zetterstrom O, and Dahlen SE (1991). 15(*S*)-hydroxyeicosatetraenoic acid (15-HETE) is the major arachidonic acid metabolite in human bronchi. *Adv Prostaglandin Thromboxane Leukotriene Res* **21A,** 441–444.

[49] Moody TW, Leyton J, Martinez A, Hong S, Malkinson A, and Mulshine JL (1998). Lipoxygenase inhibitors prevent lung carcinogenesis and inhibit non-small cell lung cancer growth. *Exp Lung Res* **24,** 617–628.

[50] Kudryavtsev IA, Golenko OD, Gudkova MV, and Myasishcheva NV (2002). Arachidonic acid metabolism in growth control of A549 human lung adenocarcinoma cells. *Biochemistry (Moscow)* **67,** 1021–1026.

[51] Shappell SB, Keeney DS, Zhang J, Page R, Olson SJ, and Brash AR

(2001). 15-Lipoxygenase-2 expression in benign and neoplastic sebaceous glands and other cutaneous adnexa. *J Invest Dermatol* **117,** 36–43.

[52] Ishida H, Takizawa M, Ozawa S, Nakamichi Y, Yamaguchi S, Katsuta T, Tanaka T, Maruyama M, Katahira H, Yoshimoto K, et al. (2004). Pioglitazone improves insulin secretory capacity and prevents the loss of beta-cell mass in obese diabetic db/db mice: possible protection of beta cells from oxidative stress. *Metabolism* **53,** 488–494.

[53] Yajima K, Hirose H, Fujita H, Seto Y, Ukeda K, Miyashita K, Kawai T, Yamamoto Y, Ogawa T, Yamada T, et al. (2003). Combination therapy with PPARgamma and PPARalpha agonists increases glucose-stimulated insulin secretion in db/db mice. *Am J Physiol Endocrinol Metab* **284,** E966–E971.

[54] Camejo G, Ljung B, and Oakes N (2001). Pharmacological treatment of insulin resistance in obesity. *Nutr Metab Cardiovasc Dis* **11,** 275–284.

[55] Dreyer C, Krey G, Keller H, Givel F, Helftenbein G, and Wahli W (1992). Control of the peroxisomal beta-oxidation pathway by a novel family of nuclear hormone receptors. *Cell* **68,** 879–887.

[56] Moller DE and Berger J (2002). The mechanisms of action of PPARs. *Annu Rev Med* **53,** 409–435.

[57] Flemmer M and Scott J (2001). Mechanism of action of thiazolidinediones. *Curr Opin Invest Drugs* **2,** 1564–1567.

[58] Murphy GJ and Holder JC (2000). PPAR-gamma agonists: therapeutic role in diabetes, inflammation and cancer. *Trends Pharmacol Sci* **21,** 469–474.

[59] Kersten S, Desvergne B, and Wahli W (2000). Roles of PPARs in health and disease. *Nature* **405,** 421–424.

[60] Fujiwara T and Horikoshi H (2000). Troglitazone and related compounds: therapeutic potential beyond diabetes. *Life Sci* **67,** 2405–2416.

[61] Straus DS and Glass CK (2001). Cyclopentenone prostaglandins: new insights on biological activities and cellular targets. *Med Res Rev* **21,** 185–210.

[62] Straus DS, Pascual G, Li M, Welch JS, Ricote M, Hsiang CH, Sengchanthalangsy LL, Ghosh G, and Glass CK (2000). 15-Deoxy-delta 12,14-prostaglandin J2 inhibits multiple steps in the NF-kappa B signaling pathway. *Proc Natl Acad Sci USA* **97,** 4844–4849.

[63] Negishi M, Koizumi T, and Ichikawa A (1995). Biological actions of delta 12-prostaglandin J2. *J Lipid Mediat Cell Signal* **12,** 443–448.

[64] Yu K, Bayona W, Kallen CB, Harding HP, Ravera CP, McMahon G, Brown M, and Lazar MA (1995). Differential activation of peroxisome proliferator–activated receptors by eicosanoids. *J Biol Chem* **270,** 23975–23983.

[65] Sun D and Funk CD (1996). Disruption of 12/15-lipoxygenase expression in peritoneal macrophages. Enhanced utilization of the 5-lipoxygenase pathway and diminished oxidation of low density lipoprotein. *J Biol Chem* **271,** 24055–24062.

[66] Wigren J, Surapureddi S, Olsson AG, Glass CK, Hammarstrom S, and Soderstrom M (2003). Differential recruitment of the coactivator proteins CREB-binding protein and steroid receptor coactivator-1 to peroxisome proliferator–activated receptor gamma/9-*cis*-retinoic acid receptor heterodimers by ligands present in oxidized low-density lipoprotein. *J Endocrinol* **177,** 207–214.

[67] Hsi LC, Wilson L, Nixon J, and Eling TE (2001). 15-Lipoxygenase-1 metabolites down-regulate PPAR gamma *via* the MAP kinase signaling pathway. *J Biol Chem* **10,** 10.

[68] Shureiqi I, Jiang W, Zuo X, Wu Y, Stimmel JB, Leesnitzer LM, Morris HZ, Fan HZ, Fischer SM, and Lippman SM (2003). The 15-lipoxygenase-1 product 13-*S*-hydroxyoctadecadienoic acid down-regulates PPAR-delta to induce apoptosis in colorectal cancer cells. *Proc Natl Acad Sci USA* **100,** 9968–9973.

[69] Shankaranarayanan P, Chaitidis P, Kuhn H, and Nigam S (2001). Acetylation by histone acetyltransferase CREB-binding protein/p300 of STAT6 is required for transcriptional activation of the *15-lipoxygenase-1* gene. *J Biol Chem* **276,** 42753–42760.

[70] Kamitani H, Geller M, and Eling T (1998). Expression of 15-lipoxygenase by human colorectal carcinoma Caco-2 cells during apoptosis and cell differentiation. *J Biol Chem* **273,** 21569–21577.

[71] Kamitani H, Taniura S, Ikawa H, Watanabe T, Kelavkar UP, and Eling TE (2001). Expression of 15-lipoxygenase-1 is regulated by histone acetylation in human colorectal carcinoma. *Carcinogenesis* **22,** 187–191.

[72] Spindler SA, Sarkar FH, Sakr WA, Blackburn ML, Bull AW, LaGattuta RG, and Reddy RG (1997). Production of 13-hydroxyoctadecadienoic acid (13-HODE) by prostate tumors and cell lines. *Biochem Biophys Res Commun* **239,** 775–781.

[73] Elstner E, Muller C, Koshizuka K, Williamson EA, Park D, Asou H, Shintaku P, Said JW, Heber D, and Koeffler HP (1998). Ligands for peroxisome proliferator–activated receptor gamma and retinoic acid receptor inhibit growth and induce apoptosis of human breast cancer cells *in vitro* and in BNX mice. *Proc Natl Acad Sci USA* **95,** 8806–8811.